NUKLEONIKA 2015;60(1):35–38
doi: 10.1515/nuka-2015-0009

ORIGINAL PAPER

DE GRUYTER
OPEN

Temperature dependence of the short-range order parameter for $Fe_{0.90}Cr_{0.10}$ and $Fe_{0.88}Cr_{0.12}$ alloys

Rafał Idczak,
Robert Konieczny

Abstract. The ^{57}Fe Mössbauer spectra for the iron-based solid solutions $Fe_{0.90}Cr_{0.10}$ and $Fe_{0.88}Cr_{0.12}$ were measured at different temperatures ranging from 300 K to 900 K. Analysis of the obtained spectra shows that the distribution of impurity atoms in the two first coordination shells of ^{57}Fe nuclei is not random and it cannot be described by the binomial distribution. Quantitatively, the effects were described in terms of the atomic short-range order (SRO) parameters and the pair-wise interaction energy with the help of a quasi-chemical type formulation introduced by Cohen and Fine. The obtained results reveal strong clustering-type correlations in the studied samples (a predominance of Fe-Fe and Cr-Cr bonds). Moreover, the changes in SRO values observed during thermal processing suggest that the distribution of Cr atoms in an α-iron matrix is strongly temperature dependent.

Key words: iron alloys • Mössbauer spectroscopy • nuclear materials • short-range order

R. Idczak✉, R. Konieczny
Institute of Experimental Physics,
University of Wrocław,
9 M. Borna Sq., 50-204 Wrocław, Poland,
Tel.: +48 71 375 9336, Fax: +48 71 328 7365,
E-mail: ridczak@ifd.uni.wroc.pl

Received: 18 June 2014
Accepted: 16 October 2014

Introduction

In the last few years, there has been much interest shown in theoretical [1–3] and experimental [4–7] determination of atomic short-range order (SRO) parameters in Fe-Cr alloys. The motivation for these studies is the fact that high-chromium ferritic/martensitic steels, containing up to 15 at.% of Cr, are candidate materials for advanced fission reactors (Generation IV), accelerator-driven systems using spallation neutron sources and fusion reactors [8, 9]. These types of steels are capable of performing reliably for a long time under high irradiation levels (total dose of 50 to 200 displacements per atom (dpa)) and at high temperatures (up to 900 K). A quantitative understanding of the mechanisms leading to the change of the properties of these steels after a long-term exposure to irradiation is, therefore, recognized to be of high importance in the safe design and operation of innovative nuclear systems. A great deal of understanding can be achieved by studying simpler model systems, such as Fe-Cr alloys in this case.

Taking the above discussion into account we decided to examine the influence of temperature on structural properties of iron-based Fe-Cr alloys. A proper investigation was performed with ^{57}Fe Mössbauer spectroscopy. This spectroscopy is a very useful tool for such studies as it can give information on the distribution of Cr atoms in the vicinity of the ^{57}Fe Mössbauer probe and then on atomic short-range order and the type of interactions between Cr and Fe atoms in the materials under consideration.

Experimental details and results

The samples of $Fe_{0.90}Cr_{0.10}$ and $Fe_{0.88}Cr_{0.12}$ alloys were prepared in an arc furnace. Appropriate amounts of the components of the alloys were melted in an argon atmosphere. The weight losses during the melting process were below 1%; hence, the compositions of the obtained ingots were close to the nominal ones. The resulting ingots were cold-rolled to the final thickness of about 0.03 mm. The ^{57}Fe Mössbauer spectra for the $Fe_{0.90}Cr_{0.10}$ and $Fe_{0.88}Cr_{0.12}$ alloys measured at different temperatures ranging from 300 K to 900 K were recorded in transmission geometry by means of a constant-acceleration POLON spectrometer of standard design, using a 60-mCi ^{57}Co-in-Rh standard source. The full width at half maximum (FWHM) of the spectral lines for the source was 0.24 mm/s. Some of the obtained spectra are presented in Figs. 1 and 2.

Each measured spectrum was fitted with a transmission integral for a sum of different six-line patterns corresponding to various hyperfine fields B at ^{57}Fe nuclei generated by different numbers of Fe and Cr atoms located in the first two coordination shells of the probing nuclei. The number of fitted six-line patterns depends on the concentration of Cr in the samples, and the values were ten for $Fe_{0.90}Cr_{0.10}$ and twelve for $Fe_{0.88}Cr_{0.12}$. The fitting procedure was carried out under the assumption that the influence of Cr atoms on B as well as the corresponding isomer shift (IS) of a subspectrum is additive and independent of the atom positions in the given coordination shell of the nuclear probe, although it can be different for atoms located in various shells. In other words, it was accepted that for each subspectrum,

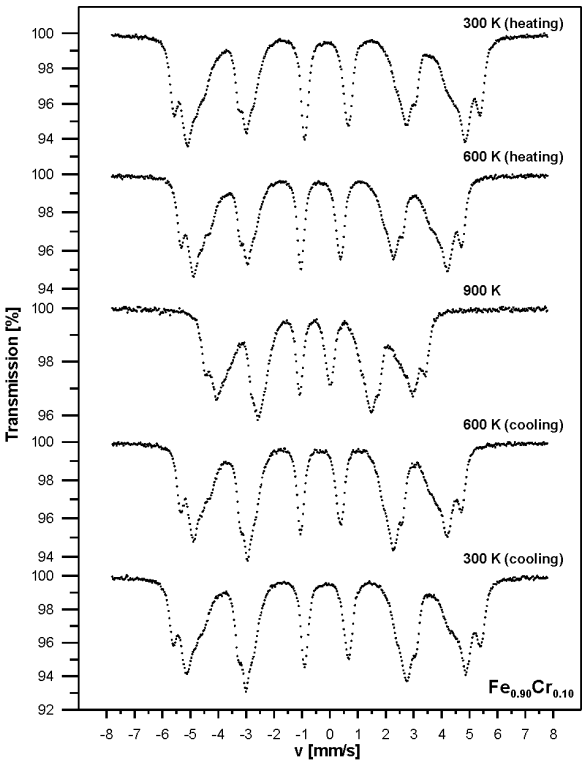

Fig. 1. The ^{57}Fe Mössbauer spectra for the $Fe_{0.90}Cr_{0.10}$ alloy at different temperatures ranging from 300 K to 900 K.

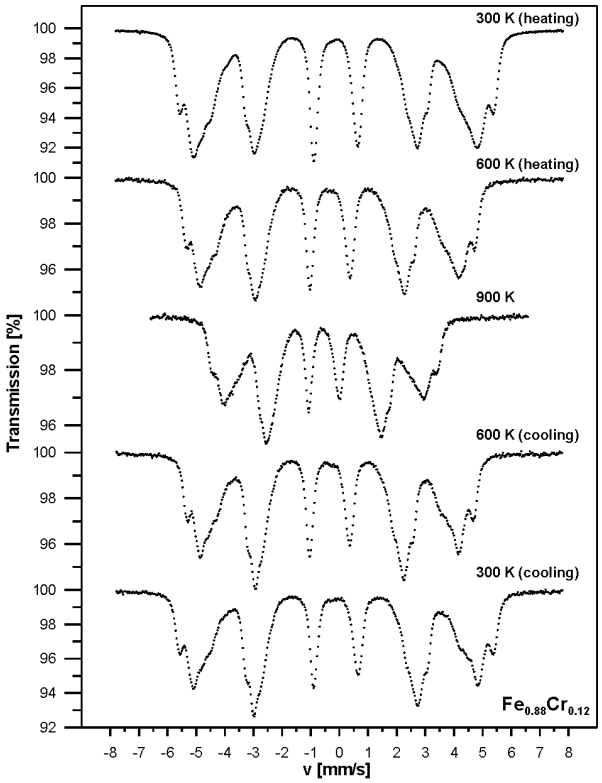

Fig. 2. The ^{57}Fe Mössbauer spectra for the $Fe_{0.88}Cr_{0.12}$ alloy at different temperatures ranging from 300 K to 900 K.

the quantities B and IS are linear functions of the numbers n_1 and n_2 of Cr atoms located in the first and the second coordination shells of ^{57}Fe, respectively. The functions can be written as follows:

$$B(n_1,n_2) = B_0 + n_1\Delta B_1 + n_2\Delta B_2 \qquad (1)$$
$$\mathrm{IS}(n_1,n_2) = \mathrm{IS}_0 + n_1\Delta \mathrm{IS}_1 + n_2\Delta \mathrm{IS}_2$$

where $\Delta B_1(\Delta \mathrm{IS}_1)$ and $\Delta B_2(\Delta \mathrm{IS}_2)$ stand for the changes of B (IS) with one Cr atom in the first and the second coordination shells of the Mössbauer probe. At the same time, we assume that the quadrupole splitting QS in a cubic lattice is equal to zero. Some results of the spectrum analysis are displayed in Tables 1 and 2.

As the main result of the analysis, effective thicknesses $T_A(n_1,n_2)$ related to the components of each spectrum were determined.

$$T_A(n_1,n_2) = \sigma_0 t_A N f c(n_1,n_2) \qquad (2)$$

where σ_0 is the maximal cross-section for nuclear γ resonance absorption, t_A denotes the thickness of the absorber, N stands for the total number of resonant absorbing atoms of ^{57}Fe per unit volume, $c(n_1,n_2)$ describes the fraction of absorbing atoms corresponding to the component under consideration and f is the Lamb–Mössbauer factor. Assuming that the Lamb–Mössbauer factor does not depend on the configuration of atoms in the surroundings of the ^{57}Fe nucleus, the fraction $c(n_1,n_2)$ can be easily calculated using the $T_A(n_1,n_2)$ values as in such cases:

$$c(n_1,n_2) = \frac{T_A(n_1,n_2)}{\sum T_A(n_1,n_2)} \qquad (3)$$

Table 1. Some of the best-fit parameters of the assumed model of the ^{57}Fe Mössbauer spectrum measured for an $Fe_{0.90}Cr_{0.10}$ alloy

T [K]	B_0 [T]	ΔB_1 [T]	ΔB_2 [T]	IS_0 (relative to α-Fe) [mm/s]	ΔIS_1 [mm/s]	ΔIS_2 [mm/s]
300	33.97(1)	–3.12(2)	–2.03(2)	0.006(7)	–0.024(2)	–0.010(2)
400	33.20(1)	–2.99(2)	–1.93(2)	–0.064(8)	–0.024(2)	–0.012(2)
500	32.21(1)	–2.99(3)	–1.94(3)	–0.137(8)	–0.024(2)	–0.012(2)
600	31.00(1)	–2.90(2)	–1.86(2)	–0.206(8)	–0.024(2)	–0.012(2)
700	29.49(1)	–2.85(2)	–1.81(2)	–0.276(8)	–0.023(2)	–0.011(2)
800	27.43(1)	–2.80(2)	–1.78(2)	–0.339(9)	–0.024(2)	–0.011(2)
900	24.76(2)	–2.77(3)	–1.75(2)	–0.397(9)	–0.029(3)	–0.011(2)

Table 2. Some of the best-fit parameters of the assumed model of the ^{57}Fe Mössbauer spectrum measured for an $Fe_{0.88}Cr_{0.12}$ alloy

T [K]	B_0 [T]	ΔB_1 [T]	ΔB_2 [T]	IS_0 (relative to α-Fe) [mm/s]	ΔIS_1 [mm/s]	ΔIS_2 [mm/s]
300	33.98(1)	–3.14(2)	–2.05(2)	0.009(8)	–0.022(2)	–0.010(2)
400	33.21(1)	–3.05(2)	–1.99(2)	–0.066(8)	–0.021(2)	–0.011(2)
500	32.21(1)	–3.04(2)	–1.98(2)	–0.140(8)	–0.020(2)	–0.011(2)
600	30.99(1)	–3.00(2)	–1.95(2)	–0.209(8)	–0.022(2)	–0.011(2)
700	29.50(1)	–2.97(2)	–1.92(2)	–0.279(9)	–0.020(2)	–0.010(2)
800	27.42(1)	–2.87(2)	–1.89(2)	–0.342(9)	–0.020(2)	–0.010(1)
900	24.84(2)	–2.82(3)	–1.81(3)	–0.396(9)	–0.019(1)	–0.015(3)

The computed $c(n_1,n_2)$ values were used to find other parameters:

$$\langle n_1 \rangle = \sum_{n_1=1}^{8} \sum_{n_2=1}^{6} n_1 c(n_1,n_2) \tag{4a}$$

$$\langle n_2 \rangle = \sum_{n_1=1}^{8} \sum_{n_2=1}^{6} n_2 c(n_1,n_2) \tag{4b}$$

$$\langle n_{12} \rangle = \langle n_1 \rangle + \langle n_2 \rangle \tag{4c}$$

where $<n_1>$, $<n_2>$ and $<n_{12}>$ are the average numbers of Cr atoms in the first, the second and two first coordination shells of the ^{57}Fe Mössbauer probe, respectively.

The average value of the short-range order (SRO) parameter for the first two coordination shells in a bcc lattice has the following form [6, 10]:

$$\alpha_{12} = 1 - \frac{\langle n_{12} \rangle}{14x} \tag{5}$$

where x is the atomic concentration of Cr. This averaging procedure is usually employed for bcc alloys, in which the first and the second neighbor distances are very close to each other [4, 6, 11].

The values of the SRO parameter α_{12} in $Fe_{0.90}Cr_{0.10}$ and $Fe_{0.88}Cr_{0.12}$ alloys calculated from Eq. (5) are presented in Figs. 3 and 4. As one can see, the positive values of the SRO parameter gave a clear evidence of clustering tendencies in studied alloys. The Cr atoms dissolved in the Fe matrix cluster into a separate Cr-rich phase. In terms of interactions, it means that the interaction between Fe and Cr atoms is repulsive (predominance of Fe-Fe and Cr-Cr bonds). Moreover, the changes of SRO values observed during thermal processing suggest that the distribution of Cr atoms in the Fe matrix is strongly temperature dependent. In particular, the significant decrease of SRO parameter values during the heating process indicates that at elevated temperatures, the Cr clusters disappear and the studied alloys become more homogeneous. In the case of the cold-rolled $Fe_{0.88}Cr_{0.12}$ alloy annealed below 700 K, the determined relatively small and constant SRO values could be associated with the frozen high-temperature state obtained just after the melting

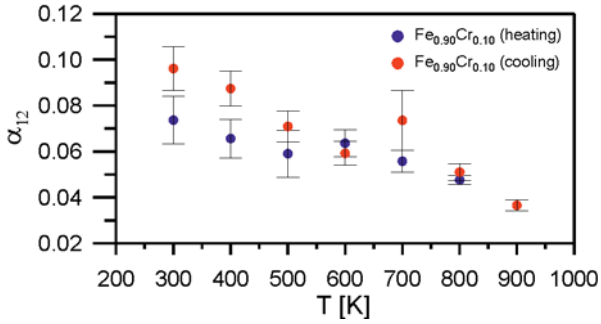

Fig. 3. The temperature dependence of the SRO parameter α_{12} for the cold-rolled $Fe_{0.90}Cr_{0.10}$ alloy.

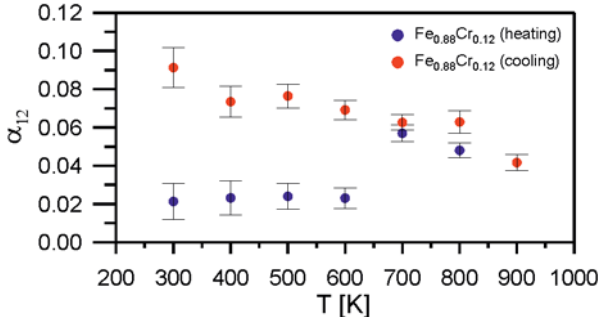

Fig. 4. The temperature dependence of the SRO parameter α_{12} for the cold-rolled $Fe_{0.88}Cr_{0.12}$ alloy.

process. As one can notice, this high-temperature state is thermally stable up to 600 K.

The interaction energy V_i of an atom in the ith coordination shell with the central atom can be defined as follows [12]:

$$V_i = \frac{V_i^{AA} + V_i^{BB}}{2} - V_i^{AB} \tag{6}$$

where V^{AA}, V^{BB} and V^{AB} are the energies for the A-A, B-B and A-B bonds, respectively. The values of the average interaction energy V_{12} of the central atom (an iron atom in our case) with atoms located in its first two coordination shells were computed using the obtained α_{12} values and the expression introduced by Cohen and Fine [12]:

$$V_{12} = -\frac{1}{2}kT\ln\left[\frac{\left(\alpha_{12} + \frac{x}{1-x}\right)\left(\alpha_{12} + \frac{1-x}{x}\right)}{\left(1-\alpha_{12}\right)^2}\right] \tag{7}$$

where k is the Boltzmann constant and T denotes the temperature characterizing the atomic distribution in the alloy under consideration. The V_{12} values, calculated for the samples during the cooling stage, are presented in Fig. 5. Negative values of V_{12} suggest that Fe-Fe and Cr-Cr bonds are more energetically favorable, thus confirming clustering tendencies. Moreover, the values of V_{12} remain constant within the experimental error, and the estimated average interaction energy V_{12} values for $Fe_{0.90}Cr_{0.10}$ and $Fe_{0.88}Cr_{0.12}$ alloys are V_{12} = –0.0148(11) eV and V_{12} = –0.0135(11) eV, respectively.

Conclusions

The obtained positive values of the SRO parameter for $Fe_{0.90}Cr_{0.10}$ and $Fe_{0.88}Cr_{0.12}$ alloys at different temperatures ranging from 300 K to 900 K gave a clear evidence of clustering tendencies in the studied materials. This result confirms previous theoretical predictions and experimental data. The changes in the SRO value observed during thermal processing suggest that the distribution of Cr atoms in the Fe matrix is strongly temperature dependent, and the significant decrease of the SRO parameter value during the heating process indicates that at elevated temperatures, the Cr clusters disappear and the studied alloys become more homogeneous. At the same time, the values of the average interaction energy V_{12} of an Fe atom with atoms located in its first two coordination shells for $Fe_{0.90}Cr_{0.10}$ and $Fe_{0.88}Cr_{0.12}$ alloys are V_{12} = –0.0148(11) eV and V_{12} = –0.0135(11) eV, respectively. In the authors' opinion, these unique experimental data could play an important role in developing and testing different models of the binary Fe-Cr alloys as well as methods for calculating the system parameters.

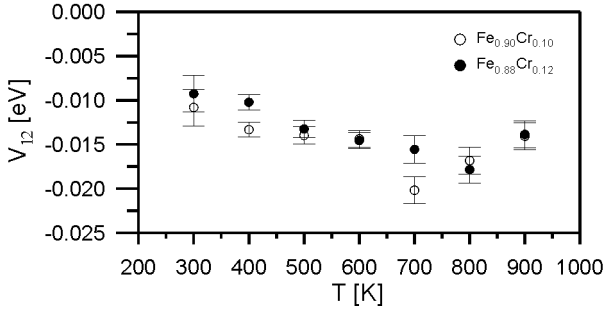

Fig. 5. The average interaction energy V_{12} as a function of annealing temperature T for the Fe-Cr alloys during the cooling stage.

Acknowledgment. The authors would like to thank Ewa Ibron for her assistance in the measurements. This work was supported by the University of Wrocław under the grant 1010/S/IFD.

References

1. Erhart, P., Caro, A., Serrano de Caro, M., & Sadigh, B. (2008). Short-range order and precipitation in Fe-rich Fe-Cr alloys: Atomistic off-lattice Monte Carlo simulations. *Phys. Rev. B*, *77*, 134206. DOI: 10.1103/PhysRevB.77.134206.
2. Bonny, G., Erhart, P., Caro, A., Pasianot, R. C., Malerba, L., & Caro, M. (2009). The influence of short range order on the thermodynamics of Fe-Cr alloy. *Model. Simul. Mater. Sci. Eng.*, *17,* 025006. DOI: 10.1088/0965-0393/17/2/025006.
3. Bonny, G., Pasianot, R. C., Malerba, L., Caro, A., Olsson, P., & Lavrentiev, M. Y. (2009). Numerical prediction of thermodynamic properties of iron-chromium alloys using semi-empirical cohesive models: The state of the art. *J. Nucl. Mater*., *385*, 268–277. DOI: 10.1016/j.jnucmat.2008.12.001.
4. Mirebeau, I., & Parette, G. (2010). Neutron study of the short range order inversion in $Fe_{1-x}Cr_x$. *Phys. Rev. B*, *82*, 104203. DOI: 10.1103/PhysRevB.82.104203.
5. Dubiel, S. M., & Cieślak, J. (2011). Short-range order in iron-rich Fe-Cr alloys as revealed by Mössbauer spectroscopy. *Phys. Rev. B*, *83*, 180202. DOI: 10.1103/PhysRevB.83.180202.
6. Idczak, R., Konieczny, R., & Chojcan, J. (2012). Atomic short-range order in $Fe_{1-x}Cr_x$ alloys studied by ^{57}Fe Mössbauer spectroscopy. *J. Phys. Chem. Solids*, *73*, 1095–1098. DOI: 10.1016/j.jpcs.2012.05.010.
7. Dubiel, S. M., & Cieślak, J. (2013). Effect of thermal treatment on the short-range order in Fe-Cr alloys. *Mater. Lett.*, *107*, 86–89. DOI: 10.1016/j.matlet.2013.05.127.
8. Mansur, L. K., Rowcliffe, A. F., Nanstad, R. K., Zinkle, S. J., Corwin, W. R., & Stoller, R. E. (2004). Materials needs for fusion, Generation IV fission reactors and spallation neutron sources – similarities and differences. *J. Nucl. Mater*., *329–333*, 166–172. DOI: 10.1016/j.jnucmat.2004.04.016.
9. Cook, I. (2006). Materials research for fusion energy. *Nat. Mater.*, *5*, 77–80. DOI:10.1038/nmat1584.
10. Cowley, J. M. (1950). An approximate theory of order in alloys. *Phys. Rev.*, *77*, 669–675. DOI: http://dx.doi.org/10.1103/PhysRev.77.669.
11. Idczak, R., Konieczny, R., & Chojcan, J. (2013). Short-range order in iron alloys studied by ^{57}Fe Mössbauer spectroscopy. *Solid State Commun.*, *159*, 22–25. DOI: 10.1016/j.ssc.2013.01.015.
12. Cohen, J. B., & Fine, M. E. (1962). Some aspects of short-range order. *Journal de Physique et le Radium*, *23*, 749–762. DOI: 10.1051/jphysrad:019620023010074901.